

ZINC STANNATE CRYSTAL STRUCTURE: AN OVERVIEW

Parihar Sarika Indersing, Research Scholar (Physics), SunRise University, Alwar (Rajasthan).
Dr. Priyanika Garg, , Research Supervisor (Physics), SunRise University, Alwar (Rajasthan).

INTRODUCTION

During the process of crystallisation by means of a solid-state reaction, zinc stannate normally undergoes a transformation from a metastable form ($ZnSnO_3$) into the stable form (Zn_2SnO_4) at temperatures in the range of 300–500 degrees Celsius. This transformation takes place at temperatures higher than 600 degrees Celsius. With high-temperature synthesis techniques such as thermal evaporation, it is difficult to generate pure Zn_2SnO_4 phase. The final result is often a mixed phase consisting of $ZnSnO_3$, Zn_2SnO_4 , and SnO_2 . The structure of the metastable $ZnSnO_3$ is that of a face-centered perovskite, while the structure of the orthostable Zn_2SnO_4 is that of a cubic spinel. The three-dimensional architectures of zinc stannate crystals are seen in figure

TYPICAL SYNTHESIS METHODS

The many methods of synthesis that have been described for ZTO nanostructures may be generally categorised as follows:

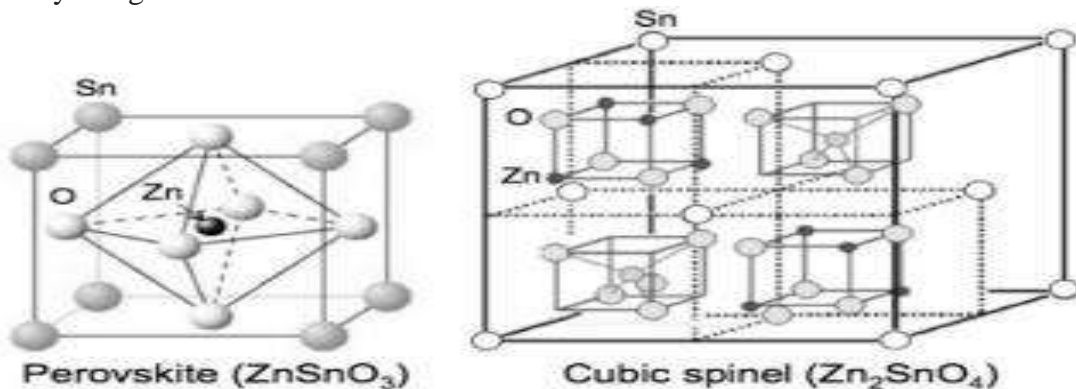


Figure: Crystal structures of zinc stannate: perovskite structure for zinc metastannate ($ZnSnO_3$) and cubic spinel structure for zinc orthostannate (Zn_2SnO_4). A single atom of each element is labeled in the structural diagrams.

Types:

- Thermal evaporation.
- High-temperature calcination.
- Mechanical grinding.
- Sol-gel synthesis

When Zn and Sn powders are subjected to thermal evaporation at temperatures over 800 degrees Celsius with or without catalysts, various ZTO nanostructures are produced. These nanostructures include nanoparticles, nanorods, and nanobelts. Many studies have reported using catalyst-assisted heat evaporation to synthesise Zn_2SnO_4 nanostructures, with Au being the most common catalyst. This method was used to produce the nanostructures. When metal oxides such as zinc oxide (ZnO), stannic oxide (SnO_2), and stannous oxide (SnO) are used as the source materials for the synthesis of ZTO nanostructures, not only is a high growth temperature required, but the final product also has a high concentration of ZnO . An ion exchange reaction between solid lithium stannate (Li_2SnO_3) and molten zinc stannate ($ZnSnO_3$) at a temperature of 350 degrees Celsius has been shown to effectively produce crystalline $ZnSnO_3$. On the other hand, the Li_2SnO_3 that was used in the ion exchange process was produced by a solid-state reaction that occurred between lithium carbonate (Li_2CO_3) and SnO_2 at temperatures ranging from 650 to 1000 degrees Celsius. Zinc chloride ($ZnCl_2$) and stannic chloride ($SnCl_4$) were used as the initial reactants in the synthesis of ZTO nanopowder that was carried out by Fu et al. This was done using a procedure known as a sol-gel method. With the addition of ammonium hydroxide (NH_4OH), the sol was transformed into a gel, which was subsequently calcined at a temperature of 600 degrees Celsius to produce the nanopowders. On borosilicate and aluminosilicate glass substrates, transparent conducting coatings of doped Zn_2SnO_4 were deposited by Kurz et al using a sol-gel process. These

coatings were conductive. In order to produce the coating solutions, the required quantities of metal chlorides or alkoxides were dissolved in ethanol at a zinc-to-tin molar ratio that ranged from 0.3 to 0.9. The coating solutions were then prepared. The creation of polycrystalline zinc stannate spinels was investigated by Nikolic' et al., who assessed the effect that mechanical stimulation had on the process of spinel synthesis. They made the discovery that the rate of synthesis of zinc stannate could be increased by grinding the material for a longer period of time, or more specifically, by extending the activation time. When the samples were stimulated for 160 minutes and then sintered at 1200 degrees Celsius for two hours, a single-phase polycrystalline zinc stannate was produced.

ZINC STANNATE

ZTO is primarily produced by high-temperature solid-state processes involving ZnO and stannic oxide (SnO₂) powders. These reactions take place at very high temperatures. The most significant limitation of this method is that it results in the loss of ZnO during the synthesis stage, which necessitates the use of one of many various heat-treatment strategies. It has also been reported that ZTO nanostructures may be synthesised by the thermal evaporation of powdered metal or metal oxide at high temperatures, as well as by the coprecipitation of zinc and tin hydroxides, followed by calcination in air. Fang et al published one of the first publications on the hydrothermal synthesis of ZTO. In this research, the authors manipulated experimental parameters such as temperature and concentration and examined how these changes influenced the formation of new phases. The hydrothermal growth technique is appealing because the nucleation and development of the crystal occur under gentle circumstances in water. This makes the process more appealing. There are reports on the control of the morphology of ZTO nanostructures producing forms such as cubes, spheres, anisotropic rods, and other similar shapes by the application of a variety of mineralizers and additives. These shapes may be produced by the nanostructures. Because the thermophysical parameters (such as temperature, concentration of reactants, and duration of crystal growth, additives, and so on) can be easily varied in solution-phase synthesis, it has been demonstrated to be an effective method for growing nanostructures with a wide range of morphologies. This may result in a better ability to regulate the thermodynamics as well as the kinetics that are involved in the process of nucleation and growth. The research into the hydrothermal development of ZTO nanostructures is currently in its infancy stage, with papers focusing on the acquired final reaction products as the primary focus. It has not yet been determined whether or not we have a complete understanding of how the nanostructures will change as the reaction proceeds. Since it is not yet feasible to actively regulate the reaction kinetics, only a handful of different morphological variants of ZTO nanostructures have been documented up to this point.

The finishing of textiles is the last stage in the chemical processing of textiles. This stage is in high demand in the modern period because it is the region in which the textile substrate experiences the greatest increase in value. Researchers have come up with a wide variety of high-demanding value-added textile materials (with features such as antimicrobial, UV-protective, fire-retardant, softened, crease proof, aroma textile, stiff fabric, odour proof textile, and so on), and they have launched these materials onto the market for customers. To achieve value-added properties of textiles, however, a huge number of synthetic compounds have been investigated in the majority of situations. 1

In the beginning of the 21st century, concerns such as eco-friendly technology, sustainability, and health dangers have become so widespread that customers are gradually shifting their desires towards items that fulfil sustainability criteria. Because of their potentially cancer-causing and poisonous properties, the majority of the synthetic chemicals used in traditional fabric finishing processes are gradually being phased out of use. Wrinkle recovery, fire retardancy, softer finish, water repellency, and other typical value additions of the textile material all need the use of a separate synthetic chemical agent for each of their respective purposes. Hence, lowering the overall cost of the process as well as the consumption of a greater amount of chemicals, energy, and time, amongst other things, is one of the most difficult difficulties facing both companies and researchers today, particularly in the present decade.

This leads to the necessity of developing multifunctional finishing, which is defined as treating textile fabrics with two or more finishing agents in a combined bath and in a single step to impart multiple functional properties together. This leads to the necessity of developing multifunctional finishing. Hence, multifunctional finishing results in savings, not only in terms of energy, but also in terms of time and water. 2 Finishing a cloth with a single agent that may impart several capabilities on the fabric is sometimes referred to as multifunctional finishing. This method makes the application simple to do while reducing the amount of water and electricity required. In addition, the amount of chemicals used in the various finishing processes will be reduced, leading to an approach that is more environmentally friendly. Nonetheless, the most difficult task is to create a material that may possibly have the capacity to represent many functions in a textile substrate. This is the true issue.

The development of such a class of multifunctional agents, ranging from bio-macromolecules to inorganic metal oxides, has been the subject of sufficient study using a variety of various technological techniques. The most well-known and rapidly developing area of study in the subject of multifunctionality is the investigation of bio-macromolecule-based technology and nanotechnology. Researchers have recently been investigating the use of a variety of waste bio-macromolecule extracts (such as the sap from banana pseudo-stems, the extract from coconut shells, the extract from pomegranate rinds, and so on) for the production of textiles that are naturally dyed, UV-protective, and fire-resistant.

In addition to this, the majority of the treated textiles exhibit antimicrobial activity against Gram-positive bacteria as well as Gram-negative bacteria.

9,10 Unfortunately, the process of extracting natural dyes is highly expensive and time-consuming. Also, natural dyes have a high add-on to the fabric, and the procedure is made somewhat more difficult by the use of mordants. Therefore, nanotechnology was elevated in the research field, and nanotechnology is a field of science that deals with matters having one or more dimensions that are less than 100 nm. Nanotechnology is currently being used in many fields in recent times, most likely in information technology, communication, paints, textiles, medicines, cosmetics, and many other fields. The use of nanostructured materials in the process of textile finishing has been more popular as of late. To the textile substrate, nanotechnology imparts specific features such as antimicrobial resistance, resistance to ultraviolet light, self-cleaning capabilities, nanoencapsulation of moisturising agents, deodorising capabilities, and the ability to repel water or oil, amongst many others.

ZINC STANNATE NANOSTRUCTURE

Organic blockers have their place, however UV blockers like TiO₂ and ZnO have a number of advantages over organic blockers, including nontoxicity and chemical stability. 16 Infusing textile substrates with other nanoparticles, such as nanosilver, zinc oxide, titanium dioxide, and others, has also been shown to have antimicrobial capabilities. The ultraviolet spectrum between 300 and 400 nanometers, which is mostly comprised of the UV A area and the UV B region, is where nanoparticles of ZnO and TiO₂ show their greatest effectiveness. TiO₂ has a maximum absorbance that mostly occurs between 290 and 320 nm, while ZnO's maximum absorbance occurs between 370 and 385 nm. 17,18 This is a disadvantage that is associated with the use of commercial UV blockers. TiO₂ nanoparticles have been investigated extensively for use as a finish that is resistant to ultraviolet light and antibacterial, but there is no evidence to suggest that they have a fire-retardant quality on their own without the addition of synergistic compounds. At the same time, ZnO has a very poor chemical stability, while TiO₂ does not have a large absorption spectrum. Because of their superior antibacterial activity, silver nanoparticles have gained significant market share in recent years.

The use of silver nanoparticles, on the other hand, has the potential to damage the surrounding ecosystem and should thus be avoided. The presence of silver in aquatic species, due to the fact that silver is a heavy metal, may result in a variety of genetic changes. Afterwards, the deposition of silver in the human body may also result in a variety of health problems. Only in the realm of antibacterial finishing has the silver nanoparticle been reported to have any effect; it does not contain any other features such as fire retardancy or resistance to UV light. Therefore, we need to develop a nanoparticle of a metal oxide kind that can provide protection

from UV rays around 300–400 nm (i.e., it will cover both the UV A and UV B regions), be nontoxic so that its deposition on organisms does not cause any detrimental effect to the ecosystem, and act also as a finishing agent that can impart multifunctional properties such as UV protection, fire resistance, antimicrobial properties, antistatic properties, and self-cleaning capabilities, amongst

Zinc stannate nanostructure is a relatively recently discovered semiconducting metal oxide. It is comparable to ZnO or TiO₂ and has a band gap that ranges from 3.8 to 4.1 eV (depending on the structure of zinc stannate), whereas ZnO and TiO₂ have band gaps that are in the range of 3.2–3.3 and 3.0–3.22 eV, respectively.

18 As UV rays strike these particles, the higher the band gap, the greater the amount of light that will be absorbed by the particles. Because of this, zinc stannate is able to cover a greater range of wavelengths while the UV absorption event is taking place. It is also known as zinc tin oxide, and in comparison to ZnO and SnO₂, it has attracted much more attention owing to the fact that it has superior optical properties, high electron mobility, high electrical conductivity, and great stability. 19 In addition, zinc stannate has been identified as a metal oxide that has both antibacterial and fire-retardant properties, making it a potentially useful substance. So, the use of zinc stannate on textile may be a highly unique method to discovering it as a chemical agent that can provide textile substrates with a wide range of multifinishes such as resistance to UV rays, antibacterial activity, and fire-retardant behaviour. The application of the finish in the nano form decreases the add-on percentage of the fabric to a far greater degree than traditional finishes, which need at least 20–30% additional coating for features such as fire retardancy. The nanostructure of zinc stannate has been investigated for use in a variety of industries, including gas sensing anode for lithium batteries; catalyst; fire retardant; antibacterial; and, most notably, as a dye destroyer owing to the photocatalytic action it has (in textiles). 20–24 The multifunctional effectiveness of the same on textile substrate has not, however, been the subject of any comprehensive research. Therefore, the primary goal of this research context is to investigate its functional effect in order to impart multiple protections of textile substrates against harmful UV rays, microorganisms, and fire, as well as to create a self-cleaning fabric that is capable of removing stains using its own mechanism.

Energy security is the foundation of contemporary communities and economies, and it is inextricably bound up with the pursuit of growth, prosperity, and peace. Without the existence of this intriguing phenomenon, the progression of human civilisation as a whole simply could not have been accomplished. Energy, and our relationship to it, has been so deeply ingrained in the development of our contemporary identity. Yet, a point that is both remarkable and significant is the fact that ever since people learned how to manufacture fire around 7.7 million years ago, the trajectory of energy growth and consumption has been multi directional. This is an interesting and crucial feature. If the earliest era indicated a lengthy time of survival and sustenance, the age of water power formed agricultural communities and structured family connections within communitarian frameworks. If this is true, then the age of sun and fire power marked the beginning of this period. However, the harnessing of wind power pushed sailing ships over vast ocean expanses, which led to the discovery of new continents and colonial politics, both of which had an impact on the fundamental structures of the current global political system.

The discovery of steam energy was a significant turning point in the annals of human history. This discovery prepared the path for the development of industry, capitalism, and economies driven by markets. The beginning of the Electrical Age, the discovery of batteries, and subsequently the discovery of electromagnetic induction, the transmission of electricity via copper wires, and the creation of electric motors finally resulted in a revolution in the way energy was transmitted. The introduction of the nuclear era marked a significant turning point in the progression of the production of energy. And just when everybody thought nuclear energy was the pinnacle of the energy matrix, two factors emerged as definite direction changers that would completely redefine the discourse and narrative on Energy Security. These factors were the potential dangers of nuclear power generation, as well as the threat of global warming and environmental degradation.

The danger posed by global warming has been appropriately labelled as a global crisis of serious proportions in the modern era, and nations all over the world have stepped up their scientific and technological efforts to locate and harness clean energy resources in the most effective and cost-effective manner possible. This study effort is also being done with this problem's context in mind as the reason for it. The researchers are concentrating on solar energy, which is a resource for clean energy, and they are striving to increase the photon collecting efficiency of dye-sensitized solar cells (DSSCs). In order to emphasise the significance of this research, it is important to provide a description and evaluation of the energy resources that are now available.

Energy today is broadly classified in to two major categories:

- Non-Renewable Energy Sources.
- Renewable Energy Source

EFFECT OF pH, REACTION TEMPERATURE, AND TIME DURATION

Experimental Preparation

0.6 grammes of LR grade zinc acetate dihydrate was dissolved in 100 millilitres of deionized water as part of a conventional hydrothermal experiment. After adding 15 ml of a sodium hydroxide solution with a concentration of 2 molar to the zinc acetate solution, the combination becomes somewhat muddy. Nevertheless, after being agitated vigorously for ten minutes, the mixture becomes homogenous. The pH meter gives this combination a reading of 12 for its pH value. After ensuring a good seal, this mother liquor was moved into an autoclave made of stainless steel and Teflon (model number Bergh of BAR 945) with a capacity of 250 milliliters, and then it was sealed. The solutions needed for the various tests were made individually and then subjected to treatment for varying amounts of time, ranging from 5 hours to 20 hours. 120 degrees Celsius, 160 degrees Celsius, and 180 degrees Celsius were selected as the temperatures to use. 13.5, 9.5, and 10.5 were chosen as the appropriate pH levels for the various studies. In order to produce solutions with the aforementioned required pH, 32 milliliters of a solution containing 2 millimeters of NaOH, 3 milliliters, and 5 milliliters of an ammonia solution are used, respectively. There are ten distinct experiments carried out, each of which differs from the others in at least one aspect of the experimental conditions. Table provides an in-depth description of the circumstances that were present throughout each of the 10 separate trials. Throughout the course of our investigations, we found that the autoclave had a pressure of around 4.8 kilograms per square meter. Experiments conducted at various temperatures will result in a shift in this pressure. When the hydrothermal treatment had been carried out for the allotted and predefined amount of time, the autoclave was let to naturally drop down to room temperature. The manufactured suspension that was found to include nanoparticles was subjected to several processes of centrifugation and washing with demineralized water and ethanol, respectively. The alcohol was fully evaporated from the centrifugate while it was drying in an oven in the laboratory.

DESCRIPTION OF CHARACTER

Structural Analysis and Considerations

The hexagonal Zinc Oxide (mineral name: zincite) was identified as the dry white powder that was analysed by X-ray diffraction (Panalytical - X'pertPro). The JCPDS Card No. 36-1451 was used to corroborate this identification. The XRD pattern of the ZnO powder that was produced is shown in figure. A comparison of the measured XRD parameters with those of the standard pattern is shown in Table, and the results show that they are equivalent to one another. The formula developed by Debye and Scherer is used to determine the average particle size (denoted by 'D') of all of the samples. The values of the lattice parameters of each and every ZNS are determined by making use of the interplanar spacing (d). When comparing various ZNS, the average particle size might vary anywhere from 23 to 64 nm. The proximity of the standard value to any given ZNS is evaluated with the help of the ratio of the lattice parameters denoted by the notation c/a.

Details of the mineralizer that was employed, the pH of the mother solution, and the experimental parameters, including temperature and the amount of time spent doing the various hydrothermal studies are included in Table.

Sample identity	Mineralizer	pH	Temperature °C	Time duration/hr
ZNS #1	NaOH	12	180	5
ZNS #2	NaOH	12	180	12
ZNS #3	NaOH	12	180	16
ZNS #4	NaOH	12	120	18
ZNS #5	NaOH	12	150	18
ZNS #6	NaOH	13.5	180	18
ZNS #7	NH ₃	9.5	120	18
ZNS #8	NH ₃	9.5	180	18
ZNS #9	NH ₃	9.5	180	18
ZNS # 10	NH ₃	10.5	180	18

CHARACTERISATION ANALYSIS OF ZINC STENNATE

The ZnO particles that had been generated were analysed using the powder X-ray diffraction (XRD) method so that the product could be identified. The XRD reflection lines have a very good correlation with the JCPDS card number 36-1451 for wurtzite zinc oxide. The figure titled "Figure" displays two diffractograms that are indicative of the ZnO nanopowders as they were manufactured. The pictures captured by the scanning electron microscope reveal a wide range of nanostructures, including nano-flowers, nanorodbunches, isolated nanotwigs with varying diameters, aspect ratios, and other characteristics, as well as agglomerations that resemble cauliflower. Figure shows the scanning electron micrographs that were acquired as a consequence of the experiments Z11–Z15 in which the concentration of NaOH was held constant (1.5 M). The shape of the ZnO nano-architecture that was formed was in the form of a flower when the concentration of zinc salt was lower. When the concentration of zinc salt increased, the shape that resembled flower petals decreased and transformed into a structure that resembled a collection of nano-needles. The ill-defined forms that result from continuing to increase the cationic concentration are shown in their entirety in Figure. When the concentration of NaOH was raised by a factor of 1M, this pattern was seen to reoccur in exactly the same way (from 1.5M to 2.5M). On the basis of the SEM images, histograms were generated to represent the various nano-architectures in their various forms. They provide a clear illustration of the diameter difference between the various nano-architectures. Figure depicts TEM photographs that were acquired for the twig-like nanoarchitecture. These pictures exhibit a uniaxially predominant growth pattern, as can be seen in the figure. This form is what is produced when the combination "Z22" is used, which is described in further depth in Table. An angular tip that is aimed towards the centre is generated at the growing end of the nanotwigs. This is often the result of the greater growth rate of the specific polar plane, as compared to the growth rate of the other non-polar planes.

RESULTS AND DISCUSSION

When the ionic strength of the system is strong, the surface charge density of the system may reach its highest point. When the charge density is at its highest point, the system's interfacial tension will be at its lowest point and vice versa. Because of the decreased nucleation energy barrier, a lower interfacial tension will ultimately result in a smaller particle size. This is because the nucleation energy barrier is lowered.

As crystals are grown from solutions, the process begins with the production of a population of nuclei that are unstable. Embryos are the name given to these nuclei that are inherently unstable. These embryos have an equal chance of either being redissolved in the solution or growing further into stable particles. Both of these outcomes are possible. In order for a particle to maintain its stability, it must reach a certain minimum radius, which is referred to as the

critical radius (R_c). The resultant competition between the surface energy required to form the embryo, i.e., $E_s = 4R^2$ (2.4), and the energy released when a spherical particle is formed, $E_v = 4R^3L/3$ (2.5), where " is the surface energy per unit area, will determine either the growth of the embryos or the thermodynamically induced redissolution of the embryo. This competition will determine whether the embryo will grow or redissolve. " denotes the density of the solid, whereas "L" stands for the heat of solution.

Due to the fact that extremely little embryos have high surface energy and are thus quickly dissolved. If the embryo (the unstable nucleus) has a volume that has the energy E_v that was described previously, then they are able to tolerate being in the solution and will be able to afford to expand into a larger nucleus. Homogeneous nucleation is the name given to the process described above in which anions and cations are present in quantities that are at or above the solubility product's upper limit.

REFERENCES

1. P. Heremans, D. Cheyns, B. P. Rand, Accounts of Chemical research, 42 (2009) 1740–1747. P.V. Kamat, J. Phys. Chem. C 111 (2007) 2834–2860.
2. V. Balzani, A. Credi, M. Venturi, Chem. Sus. Chem. 1 (2008) 26–58.
3. X. Hu, K. Huang, D. Fang, S. Liu, Materials Science and Engineering B 176 (2011) 43–435.
4. Y. Li, X. Zheng, H. Zhang, B. Guo, A. Pang, M. Wei, Electrochim. Acta 56 (2011) 9257–9261.
5. S. S. Kanmani, K. Ramachandran, and S. Umapathy, International Journal of Photoenergy 2012 (2012) Article ID 267824, 8 pages.
6. C. Justin Raj, S.N. Karthick, K.V. Hemalatha, M.K. Son, H.J Kim, K. Prabakar, J. Sol-Gel Sci. Tech. 62 (2012) 453–459.
7. Chen H, Duan Z, Lu Y.G, Pasquier A. D, Journal of Electronic Materials 38 (2009) 1612– 1617.
8. K. Sayama, H. Sugihara, H. Arakawa, Chem. Mater. 10 (1998) 3825–3832.
9. S. Rani, P. Suri, P.K. Shishodia, R.M. Mehra, Sol. Energy Mater. Sol. Cells 92(2008) 1639– 1645.
10. M. Sima, E. Vasile, M. Sima, Thin solid films 520 (2012) 4632–4636. A. Kay, M. Gratzel, Chem. Mater. 14 (2002) 2930–2935.
11. H. Zheng, Y. Tachibana, K. Kalantar-Zadeh, Langmuir 26 (2010) 19148–19152. S. Mori, A. Asano, J. Phys. Chem. C 114 (2010) 13113–13117.
12. T.H. Meen, W. Water, W.R. Chen, S.M. Chao, L.W. Ji, C.J. Huang, J. Phys. Chem. Solids 70 (2009) 472–476.
13. M.C. Kao, H.Z. Chen, S.L. Young, Thin solid films 519 (2011) 3268–3271. M.A.A. Aviles, Y. Wu, J. Am. Chem. Soc. 131(2009) 3216–3224.
14. B. Tan, E. Toman, Y. Li, Y. Wu, J. Am. Chem. Soc.129 (2007) 4162–4163.
15. T.L. Villarreal, G. Boschloo, A. Hagfeldt, J. Phys.Chem. C 111 (2007) 5549–5556.